Applied Catalysis B: Environmental 160–161 (2014) 365–373

Contents lists available at ScienceDirect

Applied Catalysis B: Environmental

journal homepage: www.elsevier.com/locate/apcatb

Ultra low temperature CO and HC oxidation over Cu-based mixed oxides for future automotive applications

Iljeong Heo[a,1], Michelle H. Wiebenga[b], Jason R. Gaudet[b,1], In-Sik Nam[a], Wei Li[c], Chang Hwan Kim[c,*]

[a] School of Environmental Science and Engineering/Department of Chemical Engineering, Pohang University of Science and Technology, San 31 Hyoja-Dong, Pohang 790-784, South Korea
[b] Optimal CAE Inc., 14492 N Sheldon Rd., Plymouth, MI 48170, United States
[c] Chemical & Materials Systems Lab, General Motors Global Research and Development, 30500 Mound Rd., Warren, MI 48090, United States

ARTICLE INFO

Article history:
Received 22 November 2013
Received in revised form 22 May 2014
Accepted 24 May 2014
Available online 2 June 2014

Keywords:
CO oxidation
Hydrocarbon oxidation
Low temperature
Ceria copper
Platinum palladium alumina

ABSTRACT

Advanced combustion technologies offer significant improvement in fuel economy as well as lower NO_x engine out emissions due to the nature of low temperature combustion; however, the lower exhaust temperature has been a major concern in the removal of hydrocarbon and CO emissions under the future emission regulation. In the present study, we discovered that cerium zirconium mixed oxide containing copper (CZCu) was more active for CO and heavy HC (i.e. C_8H_{10}, and $C_{12}H_{26}$) oxidation at below 130 °C than a platinum group metal (PGM)-based alumina catalyst under simulated diesel exhausts including NO and H_2O. The CZCu catalyst, however, was relatively inactive for the oxidation of light HC such as C_3H_6. The CZCu catalyst suffered from significant deactivation upon hydrothermal aging at 750 °C, and XRD and DRIFTS suggest that the deactivation could be due to the particle size growth of CuO retarding the formation of carbonyl on Cu upon the hydrothermal treatment. However, with smart integration of CZCu catalyst into the PGM-based catalyst the hybrid catalyst system provides opportunities for cost-effective as well as better performing aftertreatment systems for advanced fuel efficient engines.

1. Introduction

With the advent of advanced combustion techniques such as homogeneous charge compression ignition engines (HCCI) or stratified lean boosted engine (SIDI), exhaust temperatures are becoming colder [1,2]. Due to the lower combustion temperature, the NO_x level in the exhaust has decreased [1,3], however, with proposed future regulations, these newly developed fuel-efficient engines will require a catalytic converter to remove NO_x, CO and hydrocarbon (HC) emissions. The exhaust gas temperature from advanced combustion technologies can be well below 200 °C; however, conventional automotive oxidation catalysts are not active for CO and/or HCs at temperatures below 150 °C. Indeed, a variety of exhaust components such as CO, NO_x, O_2, H_2O and HCs compete with each other onto the surface of the catalyst to be adsorbed and reacted, resulting in the further decrease of the catalyst activity [4]. In the current diesel aftertreatment systems, platinum group metal (PGM) based catalysts (i.e. PtPd/alumina) have been widely used for HC and CO oxidation, but Pt suffers from self-poisoning by CO, which profoundly reduces performance at temperatures below 200 °C [5,6]. One strategy to overcome this challenge is to develop a better CO oxidation catalyst which can eliminate CO more effectively, removing this inhibiting factor from the Pt–Pd-based catalyst and allowing it to be less affected by CO.

Ceria based catalysts have been known to be active for CO oxidation at low temperatures [7–9]. Zheng et al. reported that a copper-cerium oxide catalyst without PGM is active for CO oxidation at low temperatures under simple feed conditions including CO and air balance [7]. Also, Cao et al. investigated a copper-cerium oxide catalyst containing zirconium for CO oxidation at low temperature in CO and O_2 feed stream without other reactants [9]. They suggested that the synergistic effect between CuO and the ceria material may play an important role in enhancing catalytic activity for low temperature CO oxidation. In addition, other reports have described interesting properties of various ceria based materials for CO as well as HC oxidation [10–13].

To develop an oxidation catalyst system for the low temperature exhaust, we have designed the catalyst to have high CO

* Corresponding author. Tel.: +1 586 986 0636; fax: +1 586 986 8697.
E-mail address: chang.h.kim@gm.com (C.H. Kim).
[1] Present address: Department of Chemical Engineering, University of Michigan, 2300 Hayward St., Ann Arbor, MI 48109, United States.

http://dx.doi.org/10.1016/j.apcatb.2014.05.045
0926-3373/

oxidation activity at low temperatures, leading to more favorable HC oxidation due to the lessened CO/HC competition over PGM-based catalysts. Based upon catalyst screening, a cerium zirconium mixed oxide with copper and an alumina based catalyst with PGM have been chosen for the catalytic CO and HC removal in the incorporated oxidation system, respectively. To investigate the feasibility of the newly developed catalyst system in the real world application, all the catalysts were evaluated under a simulated diesel exhaust condition as well as aged under accelerated aging cycle that has been widely accepted in the automotive industry.

2. Experimental

2.1. Catalyst preparation

According to the synthesis methods described elsewhere [9,12], two types of ceria-based mixed oxides containing copper were prepared. Ten gram each of $Ce_{0.8}Zr_{0.2}O_2$ (CZ) and $Ce0_{.6}Zr_{0.15}Cu_{0.25}O_2$ (CZCu) powder were prepared via the coprecipitation method [9]. Calculated amounts of Ce nitrate ($Ce(NO_3)_3{\cdot}6H_2O$), Zr nitrate ($Zr(NO_3)_2{\cdot}xH_2O$), and Cu nitrate ($Cu(NO_3)_2{\cdot}3H_2O$) were dissolved in 300 ml of H_2O at room temperature. Under vigorous stirring, 1 M NaOH was added to the metal precursor solution until the solution reached a pH of 10 to obtain precipitates. After mild stirring of the solution with the precipitates for 18 h, the heterogeneous solution was heated up to 80 °C for 2 h and washed with 3 L of hot water. The as-made powder was dried at 110 °C overnight, followed by calcination at 400 °C for 4 h.

$Ce_{0.61}Fe_{0.3}Cu_{0.09}O_2$ (CFCu) was prepared by the urea nitrate combustion method [12]. 13.39 g of urea was dissolved into 28 ml of H_2O with calculated amounts of Ce nitrate, Fe nitrate ($Fe(NO_3)_3{\cdot}9H_2O$) and Cu nitrate for obtaining 10 g of mixed oxide powder. When a blue-brown transparent solution was obtained, the solution was heated up to 80 °C until a viscous gel formed. After drying it overnight, the very viscous gel was separated into many crucibles and was calcined in a muffle furnace at 550 °C with temperature ramping as slow as 1 °C/min to prevent sudden combustion of the gel.

1.5 wt% PtPd/alumina (Pt:Pd = 7:1) benchmarked in the present study was set as the standard catalyst denoted as 1.5PtPd/Al and prepared by a wetness incipient impregnation method [14]. Commercial γ-alumina (CATALOX® SBa-200, Sasol) was employed for this catalyst.

Since the ceria based materials prepared in this study have their own densities, it was then necessary to fabricate the catalysts with the same amounts of PGM in the same volume of each catalyst to keep space velocities consistent during the course of the reaction. According to bulk powder densities of two ceria mixed oxides as listed in Table 1, the same amounts of Pt and Pd as those in the standard catalyst (1.5PtPd/Al) were loaded onto a specific volume of each metal oxide support by the wetness incipient impregnation method. The as-made catalyst powder was dried at 110 °C overnight, then calcined at 500 °C for 2 h.

To determine the thermal stabilities of the catalysts, the catalysts were hydrothermally aged in an oven at 750 °C for 72 h with 10% H_2O in air, which is widely used for accelerated aging protocol in automotive application [15]. This aging protocol simulates the catalyst mileage greater than 120,000 mile under diesel exhaust conditions including diesel particulate filter (DPF) regeneration events during the full usage of vehicle life [15]. Aged catalysts were denoted by '*a*-'. For example, *a*-1.5PtPd/CZCu indicates the aged 7Pt–1Pd/CZCu including same amounts of Pt and Pd as in 1.5 wt% 7Pt–1Pd/alumina (1.5PtPd/Al).

2.2. Activity measurements

For catalytic activity measurements, 0.1056 ml of catalyst powder was charged in a packed bed quartz tube reactor (o.d. 3/8 in.). The oxidation activity over each catalyst was measured over a temperature range from 125 to 300 °C while increasing the temperature stepwise by 25 °C with a 5 °C/min ramp rate under simulated diesel exhaust conditions. At each reaction temperature, the catalysts were held for 30 min in continuous feed stream to obtain the steady-state signal. The concentrations of the gaseous feeds, 500 ppm CO, 260 ppm C_3H_6, 90 ppm C_3H_8, 112 ppm $C_{12}H_{26}$, 83 ppm C_8H_{10}, 200 ppm NO, 8% O_2, 8% H_2O and N_2 (balance), were regulated by mass flow controllers or syringe pumps and fed to the reactor through heated stainless steel lines at 165 °C. Note that heavy HC refers to a mixture of 67% *n*-dodecane ($C_{12}H_{26}$) and 33% *m*-xylene (C_8H_{10}) as molar ratio which was used to represent unburned hydrocarbons in diesel exhaust. Two syringe pumps were used to evaporate liquid H_2O and heavy HC into the main feed stream. The total reactant flow rate was 300 ml/min, corresponding to a space velocity of about 170,000 h^{-1}. The inlet and outlet gas concentrations were monitored by a Nicolet Nexus 670 Fourier Transform Infrared (FT-IR) analyzer equipped with a 2 m gas cell for gas-phase analysis using a quant method calibrated at 940 Torr and 165 °C for the cell. A pressure controller at the outlet of the FT-IR was used to maintain the pressure inside the gas cell at 940 Torr.

2.3. Catalyst characterizations

The microstructures of the ceria based materials have been determined by X-ray diffraction analysis (D5000 Diffraction System). The XRD data were collected from $2\theta = 10$ to 90° with Bragg Brentano mode using Cu *K*-alpha radiation at 40 kV and 50 mA. The surface areas of the material prepared have been measured by N_2 isotherm with BET equation (ASAP2020, Micromeritics).

The active sites in CZCu and 1.5PtPd/CZCu were investigated using in-situ diffuse reflectance infrared Fourier transform spectroscopy (DRIFTS) under CO at room temperature (Nicolet Nexus 670 FT-IR). Each sample was diluted with KBr to a mass ratio of 1:5 between sample and KBr. CO adsorption modes were observed for both oxidized surfaces and reduced surfaces. In the oxidized surface case, the sample was heated to 350 °C in 10% O_2/He and held for 1 h, purged for 10 min with He, and cooled to 30 °C in He. In the reduced surface case, the sample was heated to 350 °C in 10% O_2/He, held for 1 h, purged for 10 min with He, treated with 5% H_2/He for 1 h, purged 10 min with He, and cooled to 30 °C in He. The IR spectra of the samples were measured as 1% CO was introduced over the course of 60 min. After 60 min, CO was removed and measurements were again taken for 60 min. Spectra are presented in Kubelka–Munk units.

3. Results and discussion

3.1. Catalyst activities for CO and HC oxidation

Initial screening includes two different mixed oxides as supports for PGM under simulated diesel exhaust condition. Fig. 1 shows CO, C_3H_6 and heavy HC oxidation activities of Pt–Pd supported ceria mixed oxide powder with copper as well as 1.5PtPd/Al (benchmarking catalyst), evaluated under the simulated condition with GHSV = 170,000 h^{-1}, closely corresponding to GHSV = 30,000 h^{-1} (monolith). The ceria based catalysts containing copper show better and/or similar performance for low temperature CO oxidation compared to the benchmarking catalyst. Table 2 illustrates the light-off temperatures of Ce-based metal oxides denoted by T_{50}, the temperature where 50% of conversion appears for CO and HC conversions.

Table 1
Physical properties of ceria based metal oxides.

Formula	Abbreviation	Bulk density (g/cm^3)	[a]Pore volume (cm^3/g)	BET surface area (m^2/g)
$Ce_{0.61}Fe_{0.3}Cu_{0.09}O_2$	CFCu	1.1	0.98	24
$Ce_{0.6}Zr_{0.15}Cu_{0.25}O_2$	CZCu	2.0	0.39	123
1.5%Pt-Pd/Al_2O_3	1.5PtPd/Al	0.7	0.71	118

[a] Apparent pore volume for wetness incipient impregnation of NMs.

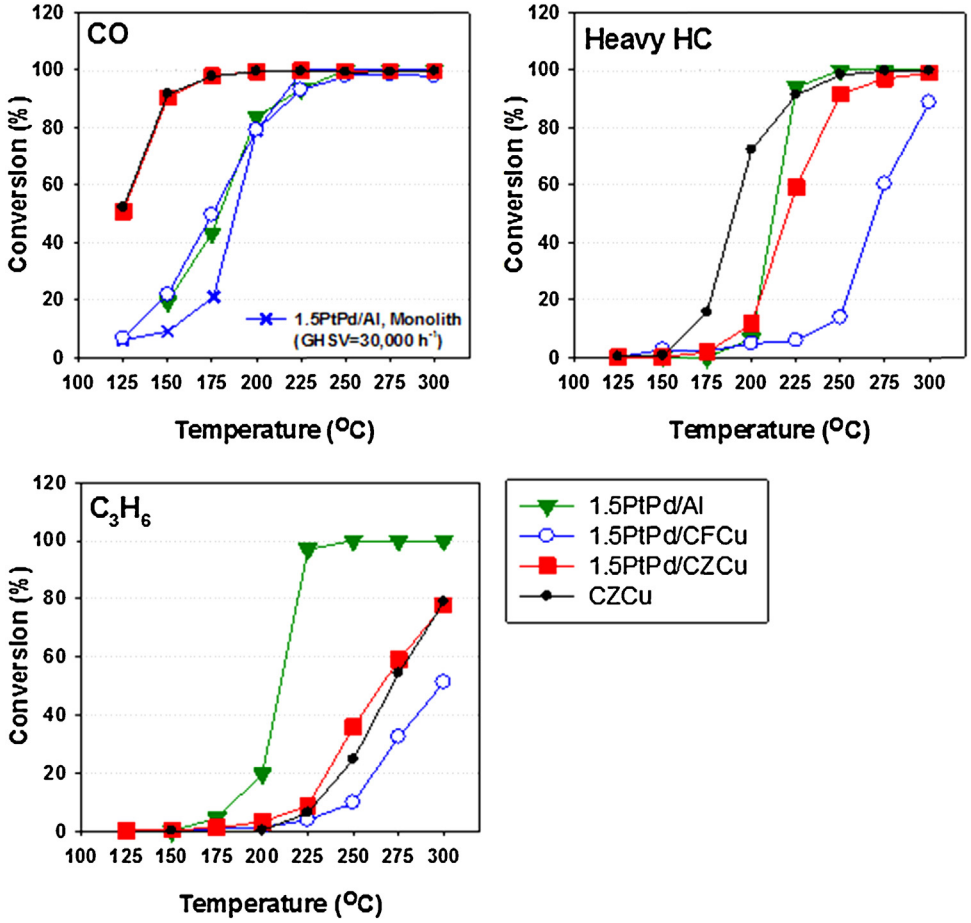

Fig. 1. Light-off curves of catalysts for CO and HCs oxidation. Feed gas composition: 500 ppm CO, 260 ppm C_3H_6, 90 ppm C_3H_8, 112 ppm $C_{12}H_{26}$, 83 ppm C_8H_{10}, 200 ppm NO, 8% O_2, 8% H_2O and N_2 balance. GHSV = 170,000 h^{-1} (powder) or 30,000 h^{-1} (monolith).

Interestingly, the CO oxidation performance of the 1.5PtPd/CZCu catalyst was significantly better than the benchmarking catalyst, 1.5PtPd/Al, and its light-off temperature (T_{50}) for CO was nearly 54 °C lower. This observation indicates that the ceria based catalyst containing copper can be a very promising catalyst for low temperature CO oxidation under the simulated diesel exhaust condition that includes H_2O, NO and HCs.

Table 2
T_{50}s of catalysts for CO, heavy HC and C_3H_6 conversions.

	T_{50}s (°C) of fresh and [aged] catalysts for reactants		
	CO	Heavy HC	C_3H_6
1.5PtPd/Al (benchmarking)	179 [193]	212 [214]	210 [213]
1.5PtPd/CZCu	125 [163]	220 [n.d.]	265 [n.d.]
1.5PtPd/CFCu	175 [167]	269 [287]	298 [298]
CZCu	124 [200]	190 [n.d.]*	271 [n.d.]*
3PtPd/Al + CZCu	129 [183]	186 [211]	187 [205]

* not determined (up to 300 °C).

Due to its low acidity, ceria has been known to promote CO oxidation [16] but not HC oxidation compared to an alumina support [17], and for this reason alumina supported PGM catalysts show better light hydrocarbon (e.g. C_3H_6) performance. In the case of heavy HC oxidation, however, the 1.5PtPd/CZCu shows comparable activity to the 1.5PtPd/Al. On the other hand, another ceria based catalyst, 1.5PtPd/CFCu, has very low activity for heavy HC oxidation at the same reaction conditions. Its T_{50} for heavy HC conversion was poor (~269 °C), and complete results are listed in Table 2.

As stated previously, the C_3H_6 oxidation activity of 1.5PtPd/CZCu is not as high as that of 1.5PtPd/Al at low temperatures. 1.5PtPd/CFCu also does not show a comparable T_{50} for C_3H_6 conversion to the benchmarking catalyst. This demonstrates that the appropriate support of PGM for light HC, such as C_3H_6, oxidation is alumina. The 1.5PtPd/CZCu is, however, still regarded as very promising candidate for a DOC component, due to its outstanding low temperature CO and heavy HC oxidation activities.

Cao et al. reported that cerium zirconium mixed oxide containing copper has high CO oxidation activity at low temperature under

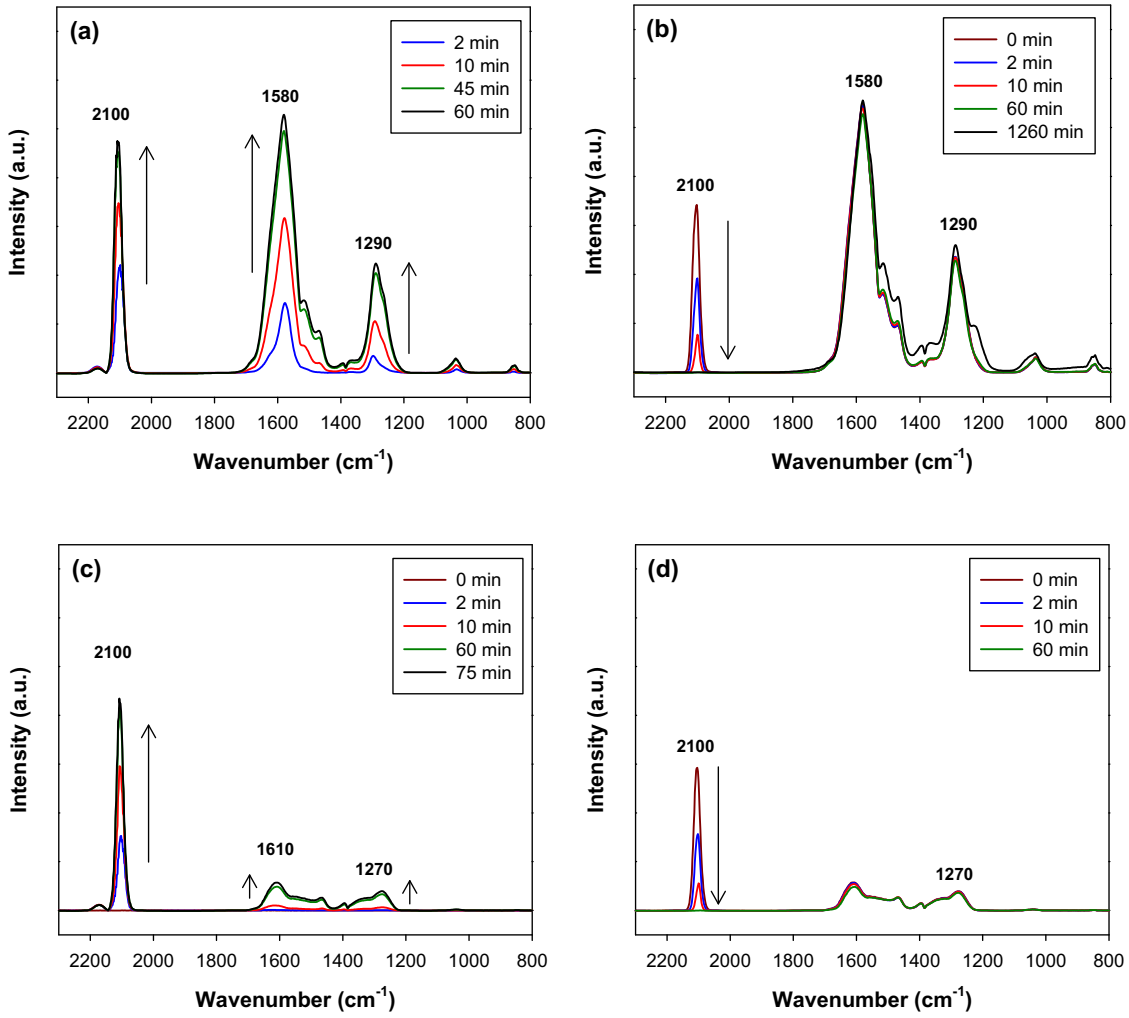

Fig. 2. IR spectra of CZCu by sequential treatment; (a) after surface oxidation and application of CO; (b) after surface oxidation and removal of CO; (c) after surface reduction and application of CO; (d) after surface reduction and removal of CO.

the simple feed condition without H_2O, HCs and NO_x [9]. The CZCu support material without PGM was evaluated under the simulated diesel exhaust condition described above. Interestingly, CZCu alone showed the exact same CO oxidation activity (T_{50} = 124 °C) that was shown over 1.5PtPd/CZCu. For heavy HC, CZCu shows even higher oxidation activity for heavy HC than in the case of 1.5PtPd/CZCu, although its light HC oxidation activity is still poor. Moreover, the T_{50} of CZCu for heavy HC conversion is about 20 °C lower than that of the benchmarking catalyst, 1.5PtPd/Al. That is an indication of a negative impact of CZCu on the active sites of PGM or vice versa. It is known that the mechanisms of CO and hydrocarbon oxidation over supported PGM-catalysts with or without CeO_2 is quite complex [16]. It clearly needs additional systematic studies to explain how CZCu was influenced on the overall rates as a function of PGM between light and heavy hydrocarbon oxidation over Pt–Pd bimetallic sites especially with the fact that the CZCu catalyst by itself is much more active for heavy hydrocarbon oxidation. Overall, we observed that the alumina is most effective support for light HC oxidation while CZCu is much more active for CO and heavy HC oxidation below 200 °C.

3.2. Active sites of CO oxidation over CZCu

Since the CZCu has demonstrated high CO oxidation activity at temperatures even below 150 °C, it is of interest to investigate the nature of active metal sites on this catalyst, thus DRIFTS was employed for this study. In the gas phase, CO has two strong vibrations of near-equal width and intensity at 2174 and 2118 cm^{-1}, along with a rotational mode which manifests as a jagged edge primarily over the 2118 cm^{-1} feature. When linearly adsorbed to a metal, these features are replaced by an intense carbonyl feature in the vicinity of 2100 cm^{-1}. Additional features, such as carbonates, carboxylates, and formates, may be observed through vibrations at energies below 1600 cm^{-1}. The locations of these vibrations are significantly influenced by the nature of the surface species to which they are bonded, and this can be used to generate more information regarding the nature of the CZCu catalyst and the effect of PGM on the interaction between CO and active surfaces.

As shown in Fig. 2, the fresh CZCu sample, after surface oxidation, generates a strong feature at 2106 cm^{-1} consistent with a Cu linear carbonyl ($Cu^{+\delta}$—CO). This feature is substantially stronger than the gas-phase CO stretching frequencies at 2174 and 2118 cm^{-1}. No $Ce^{+\delta}$—CO feature was observed, which would be present near 2160 cm^{-1}; this feature is not typically formed at room temperature [18]. The strong features at 1580 and 1290 cm^{-1} are consistent with the C═O stretch and C—O stretch, respectively, of a bidentate carbonate on Ce (Ce—O—O—CO). The weak features at 1035 and 849 cm^{-1} can be attributed to additional vibrational modes of bidentate carbonate on Ce. Weak features at 1518, 1470, and 1290 may be attributed to small amounts of monodentate and

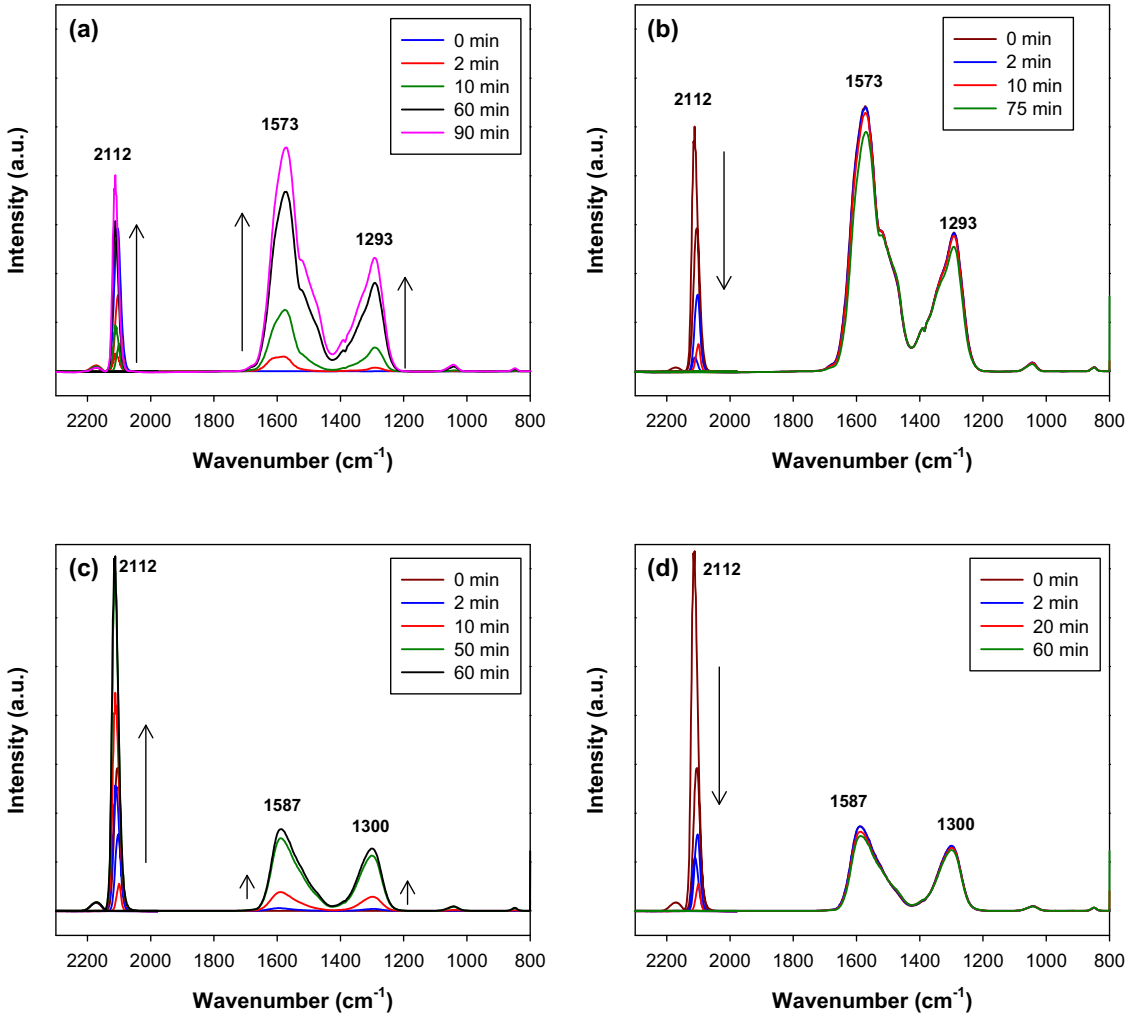

Fig. 3. IR spectra of 1.5PtPd/CZCu by sequential treatment; (a) after surface oxidation and application of CO; (b) after surface oxidation and removal of CO; (c) after surface reduction and application of CO; (d) after surface reduction and removal of CO.

multidentate carbonate on Ce. After CO is removed, the carbonyl peak rapidly dissipates, while the bidentate carbonate features remain, indicating strong adsorption.

After surface reduction, the Cu carbonyl again appears, but the intensity of this feature is significantly reduced. Notably, the carbonate features at 1610 and 1270 cm^{-1} are extremely small, as the reduced surface does not present sufficient oxygen to produce as many carbonates. As in the case of the oxidized surface, removal of CO causes the carbonyl to dissipate rapidly while the carbonates remain. The carbonyl position does not change; a shift to lower energy of 10–50 cm^{-1} would be expected if Cu^0—CO were observed.

It was considered that CO may form both carbonyls and carbonates on either Cu^0 or $Cu^{\delta+}$, in which case the oxidized surface and reduced surface should each have similar relative intensities of carbonyl and carbonate. It was also considered that CO may form carbonyls on metallic Cu^0 and carbonates on $Cu^{\delta+}$, in which case the reduction of the surface would result in an increase in carbonyl intensity and consequent decrease in carbonate intensity, as Cu is reduced to a metallic state. Neither of these cases hold true, however, as the reduced surface has a carbonyl intensity approximately 90% of the oxidized surface after CO saturation, and a carbonate intensity approximately 10% of the oxidized surface. The decreased intensity of the carbonyl peak on the reduced surface, and its position some 50–100 cm^{-1} less than anticipated for a Ce^0 carbonyl, indicate this feature is a $Cu^{\delta+}$ carbonyl.

The PtPd/CZCu sample produces a carbonyl at 2112 cm^{-1} and bidentate carbonate at 1573 and 1293 cm^{-1}, as shown in Fig. 3. As in the case of the PGM-free CZCu, the carbonyl rapidly dissipates after CO is removed, while the carbonate features remain. Additionally, the carbonate features are of much smaller intensity when formed on the reduced surface. No carbonyl either on Pt or Pd is observed, which would be visible at 2123 cm^{-1} after oxidation ($M^{\delta+}$—CO) and at 2069 cm^{-1} after reduction (M^0—CO), and which would not desorb after the removal of CO, due to the strong binding of CO to Pt or Pd at room temperature. However, the Cu carbonyl is observed to shift to 2112 cm^{-1}, indicating possible interaction among Pt, Pd and Cu. Consequently, the presence of Pt and Pd may not be beneficial to the oxidation of CO on the CZCu.

3.3. Hydrothermal stability and deactivation of catalysts

To investigate the hydrothermal stability of the catalyst, all the catalysts were treated in an oven at 750 °C for 72 h in flowing air with 10% H_2O, which simulates the field aging of the catalyst by diesel exhaust (>120,000 mile).

Fig. 4 shows CO and HC conversions over four types of aged catalysts, a-1.5PtPd/Al (benchmarking), *a*-1.5PtPd/CZCu, *a*-1.5PtPd/CFCu and *a*-CZCu. In the case of *a*-1.5PtPd/Al, the light-off curve for CO conversion is shifted to a slightly higher temperature by aging while its hydrocarbon oxidation activities are maintained

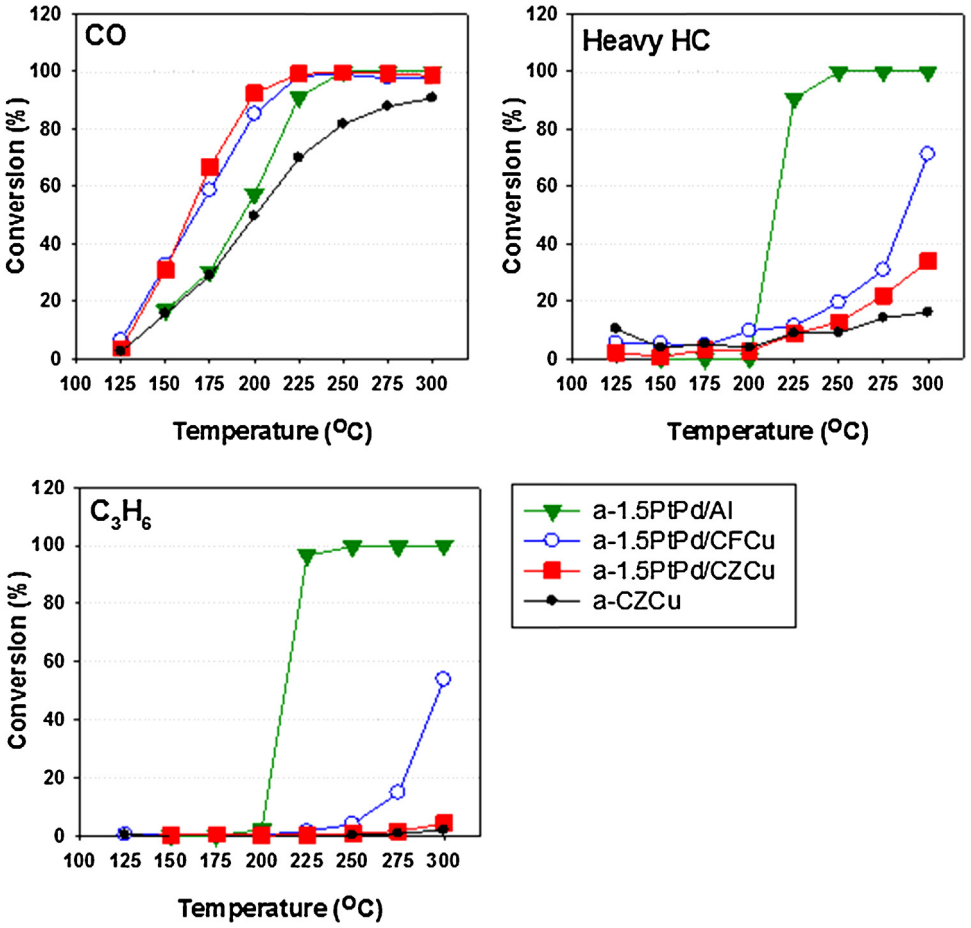

Fig. 4. Thermal stability of catalysts upon hydrothermal aging. Catalyst aging: 750 °C for 72 h with 10% H_2O in air. Feed gas composition: 500 ppm CO, 260 ppm C_3H_6, 90 ppm C_3H_8, 112 ppm $C_{12}H_{26}$, 83 ppm C_8H_{10}, 200 ppm NO, 8% O_2, 8% H_2O and N_2 balance. GHSV = 170,000 h^{-1}.

without significant change. This may indicate that Pt and Pd are stable on the surface of alumina after the hydrothermal aging employed in this study. On the other hand, all the ceria based catalysts containing copper and/or Pt and/or Pd metal particles are seriously deactivated upon hydrothermal aging. Among them, the most significant deactivation is observed over *a*-CZCu. In addition, *a*-1.5PtPd/CZCu also apparently loses its oxidation activities for CO and HC oxidation compared to its fresh counterpart. Particularly, T_{50}s of both catalysts for C_3H_6 and heavy HC conversions are not observed in the temperature range (up to 300 °C) covered in the present test protocol. However, *a*-1.5PtPd/CZCu still shows the highest activity for CO oxidation among the catalysts tested. Interestingly, another catalyst containing copper, *a*-1.5PtPd/CFCu, shows better activity maintenance upon aging, compared to the Cu-based catalyst; T_{50}s for both CO and HC oxidation were not significantly shifted to higher temperatures. This observation suggests that ceria could have played a major role in the loss of active Cu sites on 1.5PtPd/CZCu during the hydrothermal aging.

It has been observed that the 1.5PtPd/Al consisting of Pt–Pd and alumina was thermally stable, while the CZCu-based catalysts are severely deactivated upon hydrothermal aging. Moreover, 1.5PtPd/CFCu revealed less deactivation than 1.5PtPd/CZCu. This suggests that significant deactivation may appear through the degradation of ceria and/or copper oxide. Therefore, we conducted BET, XRD and DRIFTS studies over the ceria based catalysts containing copper to identify the primary cause of hydrothermal deactivation.

As listed in Table 3, BET surface areas (SA) of 1.5PtPd/CZCu, 1.5PtPd/CFCu, CZCu, and CZ were decreased by catalyst aging. The most apparent decrease of the BET SA is observed over *a*-CZCu; almost 95% of the SA is lost upon aging. On the other hand, *a*-1.5PtPd/CFCu shows the least decrease of the BET SA (50% loss) among the ceria based catalysts examined. These results are closely related to the trend of the deactivation over the three types of catalysts shown in Fig. 4. This implies that the decrease in BET surface area of the aged catalysts plays a major role in their deactivation. For the case of CZ without Cu species, the surface area decreased from 171 to 59 m^2/g (65% loss) showing better surface area maintenance compared to the case with CZCu with Cu (95% loss). To understand the role of Cu species, the phase of ternary system (Cu—Ce—Zr) needs to be further investigated; however the Cu clearly has shown a destabilizing effect on the CZ solid solution. For stabilizing the CZ material, various promoters were studied in early 1990s. For example, Jen and his co-workers reported that the addition of Pr further improves the surface area maintenance of CZ [19]. Modern three-way catalysts contain additional surface and bulk promoters for improved thermal stability [20]. Having known this, the activity

Table 3
BET surface area of fresh and aged catalysts.

	Surface area (m^2/g)		Surface area loss (%)
	Fresh	Aged	
1.5PtPd/CZCu	87	13	85
1.5PtPd/CFCu	24	12	50
CZCu	123	6	95
CZ[a]	171	59	65

[a] Cerium zirconium oxide (Ce:Zr = 4:1).

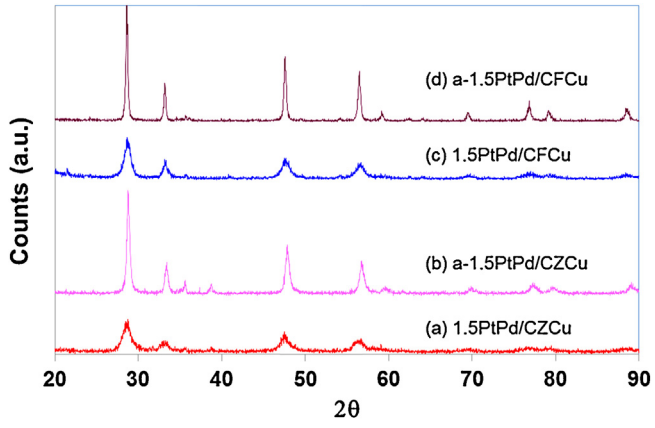

Fig. 5. XRD patterns of (a) fresh-1.5PtPd/CZCu (b) aged-1.5PtPd/CZCu, (c) fresh-1.5PtPd/CFCu and (d) aged-1.5PtPd/CFCu catalysts.

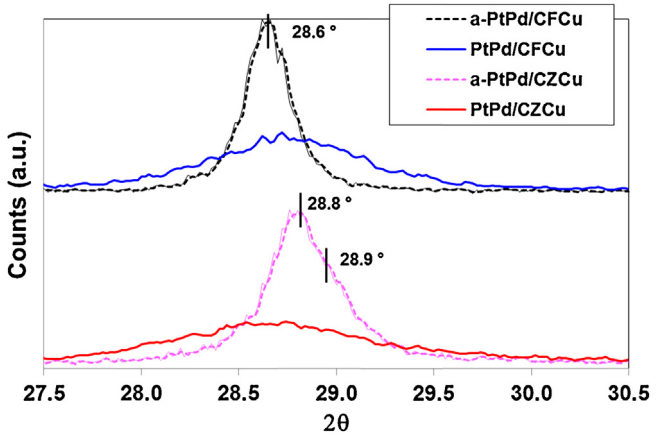

Fig. 6. XRD patterns of (solid top) fresh-1.5PtPd/CZCu (dotted top) aged-1.5PtPd/CZCu, (solid bottom) fresh-1.5PtPd/CFCu and (dotted bottom) aged-1.5PtPd/CFCu catalysts.

maintenance of CZCu could be further improved by incorporating those promoters such as Pr, Y, La, Nd, or La into the CZ solid solution.

The detailed property changes over the catalysts during the hydrothermal aging were further investigated by XRD and in-situ DRIFTS studies. As shown in Fig. 5, XRD peaks attributed to a homogeneous phase of mixed oxides in 1.5PtPd/CZCu and 1.5PtPd/CFCu catalysts are observed at between 28 and 30°, and they become more intense after catalyst aging, indicating particle growth of the solid solution. With a better resolution (Fig. 6), particularly the XRD peak of the CeO_2—ZrO_2 mixture is located at 28.6° of 2θ, which becomes narrower and shifts to 28.8° after aging suggesting the

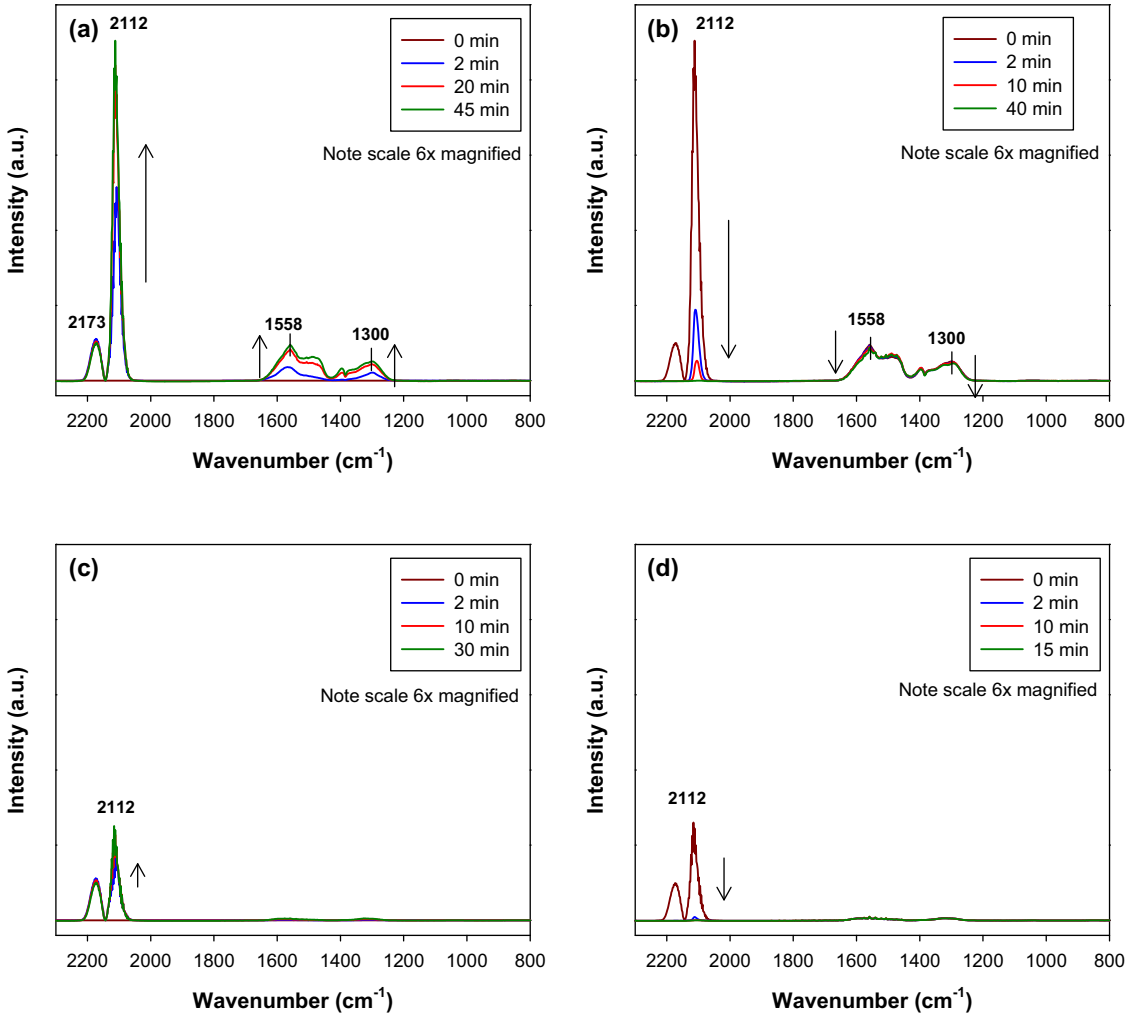

Fig. 7. IR spectra of *a*-CZCu by sequential treatment; (a) after surface oxidation and application of CO; (b) after surface oxidation and removal of CO; (c) after surface reduction and application of CO; (d) after surface reduction and removal of CO.

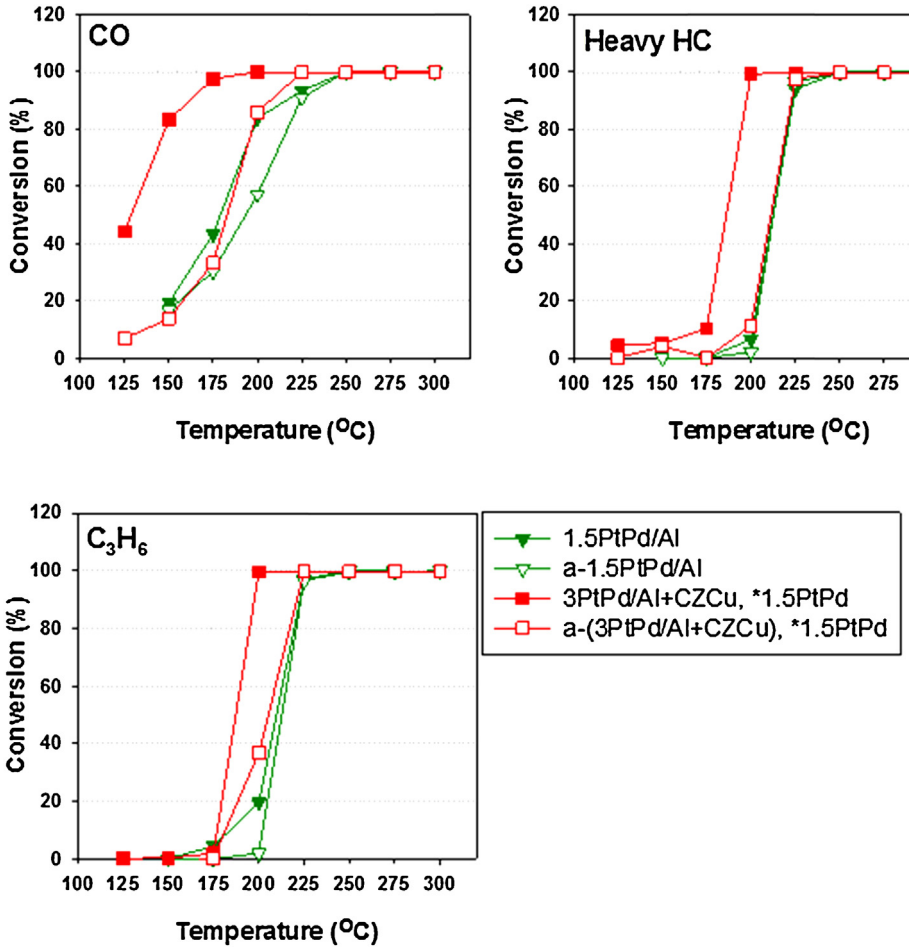

Fig. 8. Thermal stability of incorporated catalyst system upon hydrothermal aging. Catalyst aging: 750 °C for 72 h with 10% H_2O in air. Feed gas composition: 500 ppm CO, 260 ppm C_3H_6, 90 ppm C_3H_8, 112 ppm $C_{12}H_{26}$, 83 ppm C_8H_{10}, 200 ppm NO, 8% O_2, 8% H_2O and N_2 balance. GHSV = 170,000 h^{-1}.

phase transition of mixed oxides. Pure CeO_2 and pure ZrO_2 have positions of diffraction at 28.5° and 29.8° of 2θ, respectively, and an atomic mixture of 4:1 Ce:Zr oxide would normally present a peak at 28.8° [21,22]. The widths of the peaks correspond to a crystallite size increase from 7.1 to 18 nm. There is no bimodal peak, indicating no significant separation of Ce—Zr oxides into large ceria and zirconia regimes. However, the shift from 28.6° to 28.8° corresponding to a reduction in crystal lattice spacing of 3.11 to 3.09 Å, indicates inadequate mixing of the Ce and Zr phases during synthesis due to the low calcination temperature, forming Ce—Zr oxide crystallites with Ce:Zr ratio on the order of 5:1 at fresh sample (Fig. 6, solid red line), and some small ZrO_2-rich regimes, which are not visible in XRD and thus must be very small. In addition, a small peak shown at 28.9° is convoluted with the major peak (28.8°) suggesting that a structural modification occurs between Ce and Zr. Kenevey et al. also observed the diffraction peak of CZ mixture shifts as a function of calcination time and temperature enhanced by Pt and Pd metals, and the phase segregation could occur with the loss of the initial phase and form multiple phases [22]. The peak at 28.8° in Fig. 6 is consistent with the peak reported for $Ce_{82}Zr_{18}O_2$ whose ratio is quite similar to 4:1. Most importantly, it is likely that the mode of Ce—Zr oxide failure is not a large segregation of Ce and Zr into separate oxide phases. The principal XRD peak assigned for CuO is shown at 35.5° (Fig. 5), and its crystallite size over the 1.5PtPd/CZCu catalyst increased significantly while there is no observable CuO phase before or after aging over Fe-containing 1.5PtPd/CFCu catalyst. The particle growth of CuO on the ceria-zirconia mixture could be associated with the surface loss, however it's not yet clear if the growth of CuO resulted in the surface area loss or destabilized CZ mixture enhanced the particle growth of CuO.

The alteration of copper state due to sintering was also identified by DRIFTS (Fig. 7). Compared to the fresh sample, the carbonyl (2112 cm^{-1}) intensity reduced by a factor of 5 and the carbonate (1558 and 1300 cm^{-1}) intensity reduced by a factor of 50 on the oxidized surface upon aging, consistent with a substantial loss of surface area and catalytic activity. The Cu carbonyl is observed to have shifted from 2106 to 2112 cm^{-1}, consistent with a slight increase in oxidation state of Cu. As before, the removal of CO causes the carbonyl to disappear and the carbonates to remain. When the surface is reduced, the carbonate feature no longer appears, and the carbonyl is substantially weakened, disappearing completely once CO is removed. This effect may be due in part to lessened contact between Cu and ceria, which matches XRD observations of increased $CeZrO_x$ and CuO crystallite sizes upon aging. Indeed, the intensity of the Cu carbonyl feature at saturation is nearly the same for the CZCu and PtPd/CZCu catalysts, and about five times less intense for *a*-CZCu, which follows a similar trend to the oxidation performance of the catalysts.

Again, the increase in size of these CuO crystallites may be a significant factor in the reduction of the activity of CZCu, but as this size increase is nowhere near as dramatic as that of the Ce—Zr oxide crystallites the loss of CZCu activity could tentatively be assigned to a consequence of the catalyst losing 85% of its surface area.

3.4. Integration of CZCu with PtPd/alumina

The fact that CZCu alone is highly active for CO and heavy HC oxidation suggests that the combination of the CZCu catalyst with 1.5PtPd/Al could improve overall performance with the use of less PGM. Since the direct contact of PGM with the CZCu surface inhibited heavy HC oxidation as discussed, individual CZCu and PtPd/Al powders were physically mixed.

3 wt% PtPd/alumina was prepared and mixed with CZCu to keep the same amount of PGM with that in the benchmarking catalyst, 1.5PtPd/Al. To prepare the hybrid catalyst system, the same amounts of CZCu oxide and 3 wt% PtPd/Al were taken and simply shaken by hand in the proportions as described in Fig. 7 so that the mixed catalyst has an equivalent amount of Pt and Pd (1.5 wt%) in the same volume of powder as the benchmarking catalyst (1.5 wt% PtPd). By this method, Pt and Pd were loaded only on the alumina to prevent the negative effect observed in Fig. 1.

As shown in Fig. 8, the light-off temperatures for the oxidation of all three components (CO, C_3H_6 and heavy HC) were lowered with the physically mixed catalyst, 3PtPd/Al + CZCu. The T_{50}s for CO/heavy HC/C_3H_6 over this mixed catalyst are 129/186/187 °C, respectively, which are 41/26/23 °C lower than those over the benchmarking catalyst. Particularly, C_3H_6 oxidation activity is highly improved by the incorporation of CZCu with 3PtPd/Al. The heavy HC conversion of the incorporated catalyst system is slightly higher than that of CZCu oxide without PGM. In a PtPd/alumina catalyst, since CO and HCs compete with each other to be oxidized over Pt and Pd, the presence of CO retards the oxidation of HCs. Here, because of fast CO oxidation over CZCu at low temperatures, inhibition by CO over those active sites on alumina seemed to be significantly reduced for C_3H_6 oxidation.

Upon hydrothermal aging at 750 °C for 72 h, the mixed catalyst, 3PtPd/Al + CZCu, shows a decrease in catalyst activity, however, its T_{50}s for CO/heavy HC/C_3H_6 oxidation are still as low as 183/211/205 °C, respectively. Even with this activity loss, these T_{50}s are still lower than those of the benchmarking catalyst; T_{50}s of aged 1.5PtPd/Al are 193/214/213 °C for CO/heavy HC/C_3H_6 oxidation.

This hybrid system has the potential to outperform the existing technology and will be more suitable for advanced fuel efficient combustion aftertreatment. However, to become a commercially viable solution the Cu-based catalyst will need to be carefully examined for its robustness, such as sulfur tolerance, in addition to thermal durability. While both Cu- and ceria-zirconia-based catalysts are not completely resistant to sulfur poisoning, the deactivation by sulfur is reversible and the activity can be recovered via conditions that a diesel engine could generate [23,24]. Cu-based technology has been commercially used for NO_x control in diesel aftertreatment and three way catalysts for gasoline applications have contained ceria-zirconia-based catalysts for many years. While it is true that any new material for automotive exhaust catalysis will need to meet strict performance guidelines, we anticipate that the impact of sulfur on CZCu should be less of a concern compared to other types of metal oxides.

4. Conclusion

A ceria based catalyst containing copper, $Ce_{0.6}Zr_{0.15}Cu_{0.25}O_2$ (CZCu), was found to be very active for CO and heavy HC ($C_{12}H_{26}$ and C_8H_{10}) oxidation at low temperatures under simulated diesel exhaust conditions. For CO oxidation, CZCu catalyst demonstrated much higher activities even below 150 °C compared to a PtPd-based alumina diesel oxidation catalyst. However, the ceria based catalyst suffered from severe deactivation upon hydrothermal aging at 750 °C for 72 h. XRD and DRIFTS suggest that the deactivation could be due to the particle size growth of CuO retarding the formation of carbonyl on Cu upon hydrothermal treatment, resulting in a decrease of BET surface area and active sites of the catalyst. The incorporated catalyst system formed by physically mixing CZCu and 3PtPd/Al showed much higher oxidation activities than either of the two components, CZCu or 3PtPd/Al, alone for CO and all types of HCs in the temperature range covered in the present study. The light-off temperatures of the mixed catalyst for CO and HC were about 50 °C and 25 °C lower than those of the benchmarking catalyst, respectively. Upon aging, the aged mixed catalyst still showed better activities for CO and HC oxidation than the aged benchmarking catalyst. Although further investigation is still necessary to improve the thermal durability of the CZCu catalysts, we believe that the hybrid system suggested in this work is a promising catalyst configuration for low temperature exhaust aftertreatment.

Acknowledgments

The authors would like to thank Michael Balogh at General Motors Global R&D for XRD results. The authors also would like to acknowledge helpful discussions with Prof. George Graham at the University of Michigan. This work was partially funded by "National Research Foundation of South Korea (No. 2013063241 "Emission Control Catalytic System for Next Generation Energy-Efficient Vehicle" and 2012R1A3A2048833 "Center for Ordered Nanoporous Materials Synthesis").

References

[1] J.E.P. Il, V. Prikhodko, J.M.E. Storey, T.L. Barone, S.A. Lewis Sr., M.D. Kass, S.P. Huff, Catal. Today 151 (2010) 278.
[2] M. Han, D.N. Assanis, S.V. Bohac, Int. J. Automot. Technol. 9 (2008) 405.
[3] S. Kimura, O. Aoki, H. Ogawa,S. Muranaka, Y. Enomoto,;1; 1999. SAE Technical Paper 1999-01-3681 (1999), http://dx.doi.org/10.4271/1999-01-3681
[4] M. AL-Harbi, R. Hayes, M. Votsmeier, W.S. Epling, Can. J. Chem. Eng. 90 (2012) 1527.
[5] Y.-F.Y. Yao, J. Catal. 87 (1984) 152.
[6] C.-H. Lee, Y.-W. Chen, Ind. Eng. Chem. Res. 36 (1997) 1498.
[7] X.-C. Zheng, S.-H. Wu, S.-P. Wang, S.-R. Wang, S.-M. Zhang, W.-P. Huang, Appl. Catal., A: Gen. 283 (2005) 217.
[8] T.-Y. Zhang, S.-P. Wang, Y. Yu, Y. Su, X.-Z. Guo, S.-R. Wang, S.-M. Zhang, S.-H. Wu, Catal. Commun. 9 (2008) 1259.
[9] J.-L. Cao, Y. Wang, T.-Y. Zhang, S.H. Wu, Z.-Y. Yuan, Appl. Catal., B: Environ. 78 (2008) 120.
[10] Y.-M. Liu, L.-C. Wang, M. Chen, J. Xu, Y. Cao, H.-Y. He, K.-N. Fan, Catal. Lett. 130 (2009) 350.
[11] H. Zhang, W. Yang, D. Li, X. Wang, React. Kinet. Catal. Lett. 97 (2009) 263.
[12] K. Sirichaiprasert, A. Luengnaruemitchai, S. Pongstabodee, Int. J. Hydrogen Energy 32 (2007) 915.
[13] R.K. Pandey, S.P. Dagade, K.M. Malase, S.B. Songire, P. Kumara, J. Mol. Catal. A: Chem. 245 (2006) 255.
[14] I. Heo, D. Yoon, B.K. Cho, I.-S. Nam, J.W. Choung, H. Chang, Appl. Catal., B: Environ 121–122 (2012) 75.
[15] M.H. Schmid, C.H. Kim, S.H. Schmieg, D.B. Brown, D.H. Kim, J.H. Lee, C.H.F. Peden, Catal. Today 184 (2012) 252.
[16] Y.Y. Yao, J. Catal. 87 (1984) 152.
[17] M.J. Tiernan, O.E. Finlayson, Appl. Catal., B: Environ. 19 (1998) 23.
[18] A. Hornés, P. Bera, A.L. Cámara, D. Gamarra, G. Munuera, A. Martínez-Arias, J. Catal. 268 (2009) 367.
[19] H.W. Jen, G.W. Graham, W. Chun, R.W. McCabe, J.P. Cuif, S.E. Deutsch, O. Touret, Catal. Today 50 (1999) 309.
[20] M. Shelef, R.W. McCabe, Catal. Today 62 (2000) 35.
[21] I. Heo, J.W. Choung, P.S. Kim, I.-S. Nam, Y.I. Song, C.B. In, G.K. Yeo, Appl. Catal., B: Environ. 92 (2009) 114.
[22] K. Kenevey, F. Valdivieso, M. Soustelle, M. Pijolat, Appl. Catal., B: Environ. 29 (2001) 93.
[23] A. Kumar, M.A. Smith, K. Kamasamudram, N.W. Currier, H. An, A. Yezerets, Catal. Today 231 (2014) 75.
[24] T. Luo, J.M. Vohs, R.J. Gorte, J. Catal. 210 (2002) 397.